STABILIZATION OF A TWO-WHEELED INVERTED PENDULUM ROBOT

Mihai Valentin PREDOI[1]*, Sergiu STRĂTILĂ[2], Catalina-Ilinca DAN[3], Roxana-Alexandra PETRE[4], Daniel-Eugeniu CRUNȚEANU[5]

In recent years, the interest in sending exploration robots on other planets, satellites or smaller celestial bodies, has increased considerably. While the now classical configuration with six wheels remains as primary option for such missions, we investigate in the present paper a simpler exploration robot, moving on only two wheels. The advantages of higher mobility in narrow spaces and lower mass come with an inconvenience: the stability of such a robot. In the present paper is investigated the stability problem of such a robot.

Keywords: Stabilized inverted pendulum, two-wheeled robot.

1. Introduction

Nowadays, mobile robots are becoming a common presence, even in space missions. They are used for various tasks, such as exploration, object manipulation, search and rescue in hard-to-reach human-accessible spaces, and entertainment, especially among young people. Legged robots have more degrees of freedom than other types of robots, making them more challenging to design and control, even though they can overcome some obstacles.

Wheeled robots require less dynamics and energy than legged robots to establish contact with the ground and provide propulsion, given their direct contact with it [1]. They also have a simpler mechanical structure, which allows for significant size reduction and higher energy efficiency.

[1]* Dept. of Mechanics, Faculty Biotechnical Systems Engineering, National University of Science and Technology Politehnica Bucharest, Romania, e-mail: mihai.predoi@upb.ro (Corresponding author)
[2] Dept. of Propulsion Systems, Faculty of Aerospace Engineering, National University of Science and Technology Politehnica Bucharest, Romania, e-mail: sergiustratila2001@gmail.com
[3] Dept. of Propulsion Systems, Faculty of Aerospace Engineering, National University of Science and Technology Politehnica Bucharest, Romania, e-mail: catalina.ilinca@yahoo.com
[4]* Dept. of Mechanics, Faculty Biotechnical Systems Engineering, National University of Science and Technology Politehnica Bucharest, Romania, e-mail: petre.roxana.alexandra@gmail.com
[5] Dept. of Propulsion Systems, Faculty of Aerospace Engineering, National University of Science and Technology Politehnica Bucharest, Romania, e-mail: daniel.crunteanu@upb.ro

Due to their advantages, such as the ability to make zero-radius turns and agility in tight and crowded spaces, the two-wheeled inverted pendulum (TWIP) robot has become a significant research subject in recent decades [2]. In recent years, an TWIP robot has become an attractive option for urban patrols or daily commuting, such as Segways, due to the increasing severity of urban traffic congestion. By improving their mobility and requiring less space, TWIP robots, like Anybots QB [3], can also be selected as service robot platforms. An TWIP robot can be used as a learning tool or as a research object for various experiments that can help future space missions, given that it represents an underactuated and nonlinear system [2].

Being underactuated, the robot has more degrees of freedom than control inputs. Dynamics can be greatly simplified by having robots with at least three wheels, which allows for static stability. A four-wheel design is also widespread; this is particularly noticeable in vehicles, as the larger support plane improves stability at high speeds [1]. However, when there are more than three wheels, the mechanism becomes too restricted, and except for flat terrain, a suspension system is necessary. Therefore, the statically unstable type of two-wheeled robots is the subject of this research. Due to their two coaxial wheels positioned on each side of an intermediate body and their center of mass being above the wheel axles, these robots are at risk of toppling over and therefore need to be actively stabilized [4].

Two-wheeled robots are still much easier to maneuver than legged ones, even though they pose a greater operational challenge than statically stable wheeled robots. Due to their wheel arrangement, which allows them to make quick turns like differential drive robots, they are extremely maneuverable [5], [1]. Their ability to spin on the spot compensates for their unstable nature. Through active stabilization, even a robot with a larger center of mass can compensate for any disturbances that could otherwise cause a statically stable robot to topple over. Due to their ability to navigate tight spaces and short hallways, two-wheeled robots can be taller and have a smaller footprint, making them ideal for indoor environments.

The manuscript is organized as follows: from the classical inverted Kapitsa pendulum studied in paragraph 2, to which we replace the controlled vertical displacement of the hinge by a controlled force, we investigate the inverted pendulum with horizontal motion of the hinge which is acted by a harmonic force, and we deduce the stability domains in paragraph 3. In paragraph 4 is investigated the two-wheels robot which is acted by controlled motor torques. The Proportional-Differential- Integral (PID) controller is described, and the practical obtained results are presented in the 5-th paragraph. All mechanical models are followed by numerical examples using Partial-Differential-Equations (PDE) solvers applied to our systems of PDE.

One objective of this study on two-wheeled robots is their motion in environments with obstacles, where robots need to accomplish additional actions.

2. The inverted pendulum stabilized by forced vertical motion

An inverted mathematical pendulum made of a material point of mass *m* at the end of a mass-less rod, stabilized by a harmonic vertical motion of the hinge was first investigated by P.L Kapitsa [6]. Many researchers developed this problem, e.g. refs. [7], [8], [9].

In this paragraph is studied an inverted physical pendulum, which is made of a rigid rod of mass *m* and length *l*, having the pivot joint moving along the vertical direction. The rod is hinged to a slider on mass *M*, which is moved by an applied vertical force *F(t)* (Fig. 1). This is a generalization of the classical Kapitsa pendulum, with forces acting the slider instead of imposed displacements.

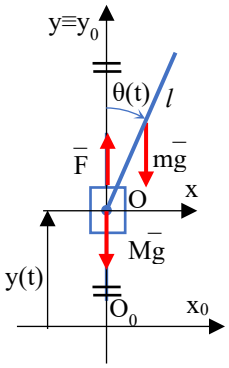

Fig. 1. The inverted pendulum with vertical hinge motion. $O_0x_0y_0$ is a fixed frame, Oxy is a moving frame

Using as generalized parameters the position *y(t)* of the hinge and the angle *θ(t)* of the rod with the vertical direction, the kinetic energy of the mechanical system is:

$$T = \frac{1}{2}(m+M)\dot{y}^2 + \frac{ml^2}{6}\dot{\theta}^2 - \frac{m}{2}l\dot{y}\dot{\theta}\sin\theta \ . \tag{1}$$

The generalized forces associated to the selected parameters are :

$$Q_y = F(t) - (m+M)g; \quad Q_\theta = mg\frac{l}{2}\sin\theta \tag{2}$$

The Lagrange equations [10] for this mechanical system can be written:

$$\begin{cases} \frac{2l}{3}\ddot{\theta} - \ddot{y}\sin\theta = g\sin\theta \\ \frac{2(M+m)}{m}\frac{\ddot{y}}{l} - \ddot{\theta}\sin\theta = \dot{\theta}^2\cos\theta + 2\frac{F(t)-(m+M)g}{ml} \end{cases} . \tag{3}$$

The classical Kapitsa approach is to consider the hinge displacement $y(t) = e\sin pt$, with a small amplitude *e* and angular frequency *p* and denoting by

$\omega_0 = \sqrt{\frac{g}{l}}$, the angular frequency of the equivalent simple pendulum. With these notations, the first of eq. (3) becomes :

$$\ddot{\theta} - \frac{3}{2}\omega_0^2\left[1 - \frac{e}{l}\frac{p^2}{\omega_0^2}\sin pt\right]\sin\theta = 0\,. \tag{4}$$

Considering small angles θ, the usual approximation $\sin\theta \approx \theta$ holds and the previous equation takes the form of a classical Kapitsa pendulum differential equation [11]:

$$\ddot{\theta} - \omega_0^2\left[1 - \frac{e}{l}\frac{p^2}{\omega^2}\sin pt\right]\theta = 0\,. \tag{5}$$

Clearly, one condition for stability applies to the hinge motion: $ep^2 > l\omega^2$.

In the following are used the differential equations (3), which are considering an applied force $F(t) = F_0 \sin pt$ moving the system and not an imposed displacement, taking into account the mass M of the slider. The nonlinear differential equations are numerically integrated using the ode45 function of Matlab [12] for the following numerical values: M = 0.3 kg , m=0.3 kg, l=0.12 m and a harmonic vertical force $F = F_0 \sin pt$ with $F_0 \in [0.2\ 5]$ N and $p = 2\pi f$, in which the forced motion frequency is in the range f = 0.25 – 5 Hz. The initial conditions used for the numerical integration are: $\theta(0) = 1° = 0.0175\ rad$; $\dot{\theta}(0) = 0\ rad/s$; $x(0) = 0\ m$; $\dot{x}(0) = 0\ m/s$.

The numerical solutions shown on Fig. 2 represent an unstable motion F_0=2N, f= 1Hz (a) and a stabilized motion for F_0=2N, f= 2Hz (b). Since the mechanical system has no damping, the motion cannot be asymptotically stable. Consequently, the system is considered stable if it corresponds to a quasi-stationary motion during the integration lapse of time.

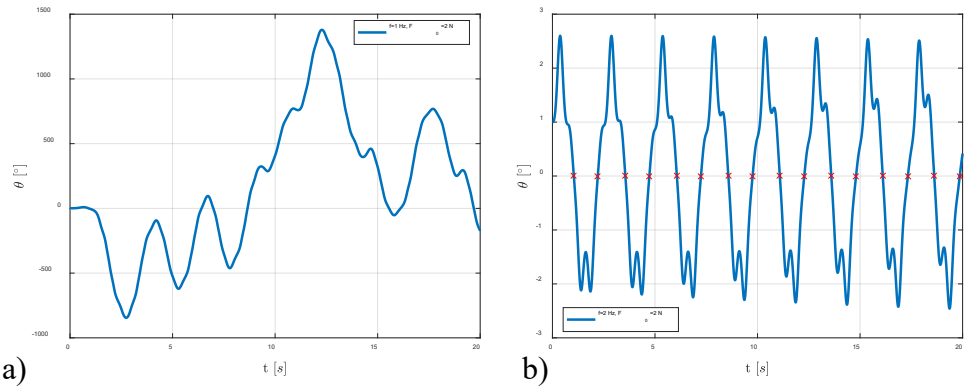

Fig. 2 The angular displacement for an inverted pendulum with F_0=2N: unstable for f=1Hz (a) and stable for f = 2Hz (b)

It is interesting to note that the spectral analysis of the signal in Fig. 2b includes peaks at 0.4 Hz, 1.6 Hz and 2.4 Hz which indicates a sort of beat phenomenon around f=2 Hz. The dependency of the stability, considered as oscillations with bounded limits, on the set of parameters (f, F_0) is shown on Fig. 3 for two initial angles θ_0 =1° and 5°. The stability boundary is a smooth curve and the stability sets are marked by dots, showing a weak influence of the initial angle.

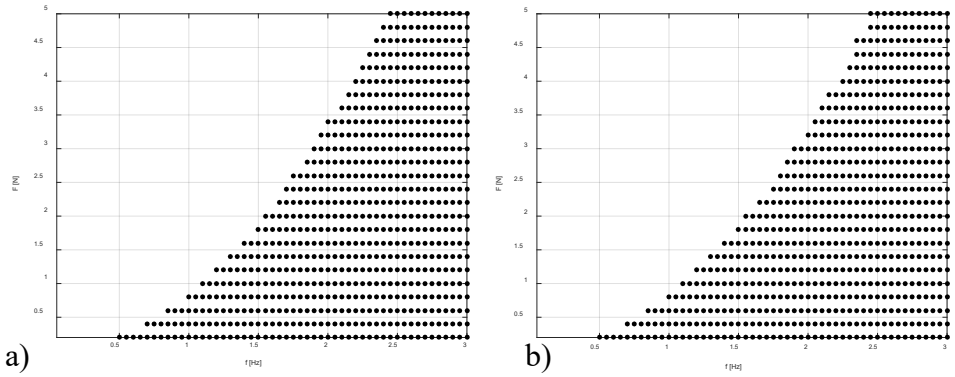

Fig. 3 Stability domain (dots) in the frequency-force analysis: initial angle θ_0 =1° (a); θ_0 =5° (b)

The stability problem for the horizontal motion of the slider will be studied in the next paragraph.

3. The inverted pendulum stabilized by forced horizontal motion

The inverted pendulum with horizontal motion of the hinge was less studied, and only a few references can be found, among which it is mentioned ref. [13].

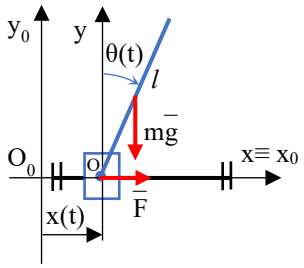

Fig. 4. The inverted pendulum with horizontal hinge forced motion. $O_0x_0y_0$ is a fixed frame, Oxy is a moving frame.

For the mechanical system shown on Fig. 4 in which the mechanical parameters are the same as in the previous paragraph, the kinetic energy is:

$$T = \frac{1}{2}(m+M)\dot{x}^2 + \frac{ml^2}{6}\dot{\theta}^2 + \frac{m}{2}l\dot{x}\dot{\theta}\cos\theta\,. \tag{6}$$

The generalized forces associated to the selected parameters are :

$$Q_x = F(t);\ Q_\theta = mg\frac{l}{2}\sin\theta\,, \tag{7}$$

in which $F(t) = F_0 \sin pt$, with F_0 [N] the amplitude of the harmonic stabilizing force and p [rad/s] its angular frequency. The Lagrange equations [10] deduced for this mechanical system can be written as:

$$\begin{cases} (M+m)\ddot{x} + \dfrac{ml}{2}\ddot{\theta}\cos\theta = F(t) + \dfrac{ml}{2}\dot{\theta}^2\sin\theta \\ \dfrac{1}{2}ml\ddot{x}\cos\theta + \dfrac{ml^2}{3}\ddot{\theta} = mg\dfrac{l}{2}\sin\theta \end{cases} \tag{8}$$

We keep the nonlinear terms in the system and the temporal solution is obtained by numerical integration using the ode45 function in Matlab [12].

As a numerical example, the same parameters were taken: M = 0.3 kg , m=0.3 kg, l=0.12 m and a harmonic horizontal force $F = F_0 \sin pt$ with F_0 = 0.2 … 5 N and $p = 2\pi f$, in which the forced motion frequency is in the range f = 0.01 – 0.5 Hz. The initial conditions used for the numerical integration are: $\theta(0) = 1° = 0.0175\ rad;\ \dot{\theta}(0) = 0\ rad/s;\ x(0) = 0\ m;\ \dot{x}(0) = 0\ m/s$.

For the particular case F_0 =2N and frequency f_1 = 0.05 Hz, a stabilized motion was obtained, as shown on Fig. 5a. On the contrary, for F_0 =2N and f_2=0.15 Hz, the motion becomes unstable (Fig. 5b).

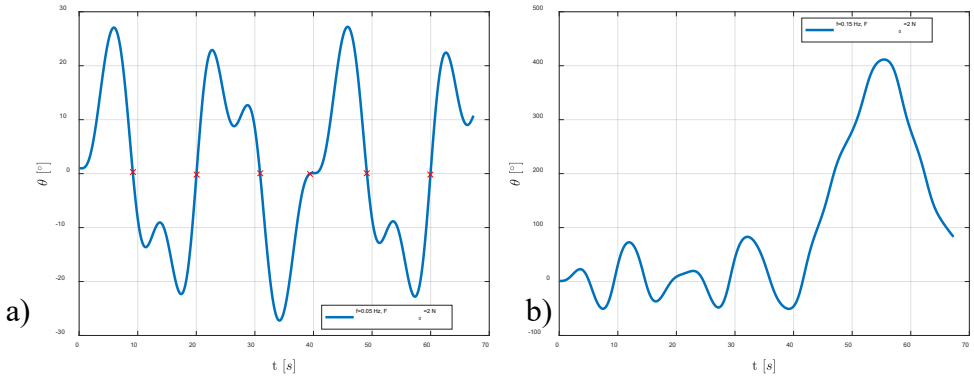

Fig. 5 Pendulum angle evolution in time: stable motion (a), unstable motion (b)

This unusual behavior, indicates the existence of stability domains influenced by the applied force and of its frequency. On Fig. 6 are plotted the stabile solutions as

a dot for each pair (F_0, f). It can be remarked that the system can be stabilized by small forces over a wider range of frequencies. As the amplitude of the force increases, the instability domain (without dots) widens, but not in a regular manner: the instability boundary a rugged curve. Moreover, the influence of the initial θ angle from 1° in Fig. 6a increased to 5° in Fig. 6b, is not important, the widening of the instability domain is limited.

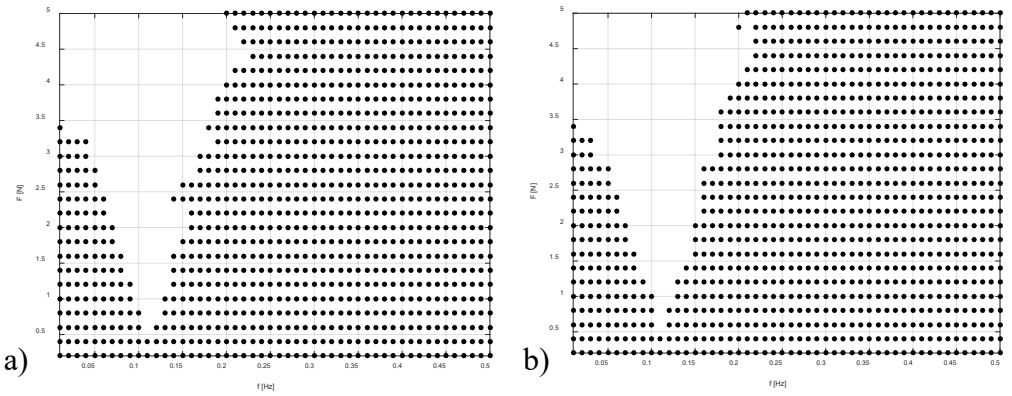

Fig. 6 Stability domain (dotted) in the frequency-force analysis: initial θ angle 1°(a) and 5°(b).

One important remark concerns the spectral analysis of the stabilized signals. For the motion shown on Fig. 5a there are two dominant frequencies: $f = 0.05$ Hz and $f_p = 0.12$ Hz. The first one is the excitation frequency, which is expected. However, the second frequency f_p, is an interesting result since this mechanical system has as natural frequency f_n=2.23 Hz for the free oscillations, which do not correspond to the identified frequency f_p.

4. The two-wheeled robot with active control

In the previous two paragraphs, was studied the stability of mechanical structures exhibiting inverted physical pendulums. However, this is a passive stabilization, requiring a permanent oscillatory acting force, which implies a large energy consumption. In view of space robots applications, a structure with two wheels and the robot body like an inverted physical pendulum is an interesting option. It requires less space for maneuvers and less energy consumption if the stability is actively controlled, acting only when possible loss of balance is detected.

The two-wheeled robot can be associated with more or less simplified models. We consider the 2-DOF model shown on Fig. 7: Two identical wheels (radius r and mass m) can roll without sliding on the horizontal surface Ox_0, with sliding coefficient μ and rolling friction coefficient s, under the action of two identical motors, each giving a torque M_m. The robot body is defined by its weight Mg,

applied at the mass center OC = *d* and its mechanical moment of inertia about the central axis Oz: J_C.

The positional parameters are the position *x(t)* of the wheels centers, relative to the fixed frame ($O_0x_0y_0$) and the pitch angle *θ(t)* of the robot's body, relative to the vertical direction (O_0y_0).

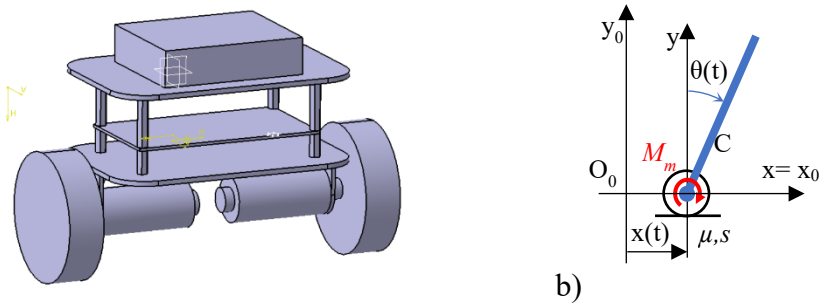

Fig. 7. The two-wheeled robot in perspective drawing (a) and the mechanical model (b). $O_0x_0y_0$ is a fixed frame, Oxy is a moving frame. The motor moment M_m is in a control loop with an inertial measurement unit (IMU) and a microcontroller ATmega328.

It is assumed that the wheels are rolling without sliding, so that the wheels rotations *φ(t)* are linked to the displacements of their centers: $x(t)=r\varphi(t)$. The kinetic energy of the robot is:

$$T=\frac{M+3m}{2}\dot{x}^2+M\dot{x}\dot{\theta}d\cos\theta+\frac{1}{2}\left(Md^2+J_C\right)\dot{\theta}^2 \tag{9}$$

The generalized forces are obtained from the virtual work of applied forces and moments $\delta W=\left[2M_m-s\left(M+2m\right)g-sMd\left(\dot{\theta}^2\cos\theta+\ddot{\theta}\sin\theta\right)\right]\frac{\delta x}{r}+\left(Mgd\sin\theta-2M_m\right)\delta\theta$.

It has been included, using the principle of d'Alembert, the influence of robot pitch motion on the normal reaction. However, for the slow motions around equilibrium positions, this term can be neglected. Consequently:

$$\begin{cases}Q_x=\dfrac{2M_m-s\left(M+2m\right)g}{r}\\ Q_\theta=Mgd\sin\theta-2M_m\end{cases} \tag{10}$$

The Lagrange equations for this model of robot become:

$$\begin{cases}\left(M+3m\right)\ddot{x}+Md\left(\ddot{\theta}\cos\theta-\dot{\theta}^2\sin\theta\right)=\dfrac{2M_m\left(\dot{\theta}\right)-s\left(M+2m\right)g}{r}\\ \left(J_C+Md^2\right)\ddot{\theta}+Md\ddot{x}\cos\theta=Mgd\sin\theta-2M_m\left(\dot{\theta}\right)\end{cases} \tag{11}$$

This system of nonlinear differential equations was integrated using an algorithm written in MATLAB. The two electric motors with reduction gears have a linear

characteristic torque-angular velocity as: $M_{m0}\left(\frac{\dot{x}}{r}\right)=M_{\max}\left(1-\frac{\dot{x}}{r\omega_{\max}}\right)$ in which M_{max} = 0.438 Nm and ω_{max}=36.65 rad/s, taken as numerical examples from the existing robot investigated in the following.

The robot is controlled by a proportional-differential (PD) control loop. The information θ and $\dot{\theta}$ are provided by an inertial measurement unit (IMU) fixed to the robot chassis. These information are used by microcontroller ATmega328 on which was programmed the code which controls the voltage applied to the two motors, providing the corresponding torque M_m:

$$M_m=M_{m0}\left(\frac{\dot{x}}{r}\right)\left[k_p\theta(t)+k_d\dot{\theta}(t)\right]. \tag{12}$$

The two constants of the PD controller are determined by successive tests, since the available torque already depends on the instantaneous angular velocity of the wheels. The mechanical properties of the robot are similar to those used in the previous paragraphs. A sliding friction coefficient $\mu>0.1$ is sufficient to provide rolling without sliding for both wheels. For the existing robot, the constructive data are summarized in Table 1.

Table 1

Robot constructive data

Wheels radius (mm)	Wheel mass (g)	Chassy mass (kg)
25	80	0.445

We determined using the CAD model shown on Fig. 7a the central moment of inertia about an axis parallel to the wheel's axis: J_C = 0.0041 kg.m^2 and we used an estimated rolling friction coefficient s=0.5 mm. The initial conditions are: $\theta(0)$ = 5°; $\dot{\theta}(0)=0$; $x=0$; $\dot{x}=0$.

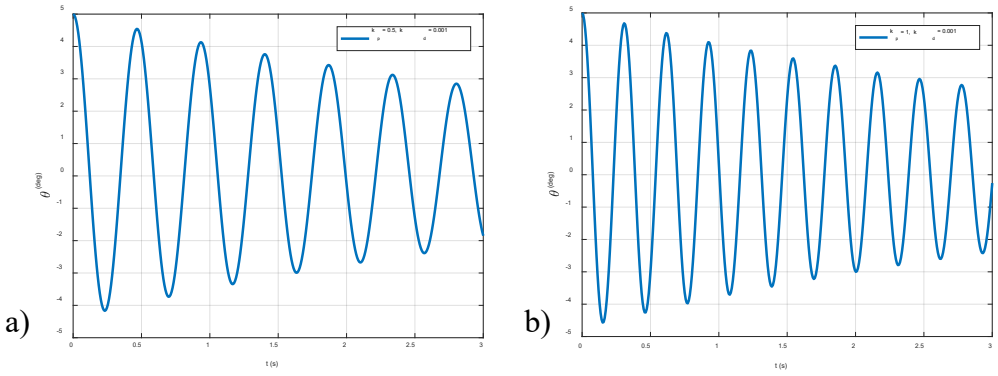

Fig. 8 Robot's inclination as function of time, for two values of k_p.

The following numerical tests were the most suggestive, for a simulation time of 3s. Using k_p=0.5 Nm/rad; k_d=0.001 Nms/rad was obtained the dependency shown on Fig. 8a.

Doubling the proportionality constant to k_p=1 Nm/rad produces the plot in Fig. 8b which indicates an increased frequency of oscillation of the robot, but the final values remains relatively constant.

The differential constant k_d was changed to k_d=0.01 Nms/rad for the same k_p values and the results are shown on Fig. 9. The strong damping effect of k_d is apparent. It can be considered that practically after 2s the robot is stabilized, which is an acceptable duration.

Moreover, the influence of k_p can be seen on the asymptotic value of the inclination, which is decreasing form 0.3° to 0.1°. It can be considered that as a minimal requirement k_p=1 Nm/rad and k_d=0.01 Nms/rad, are providing acceptable results. Certainly, higher values can get the final value of the inclination closer to zero and much faster.

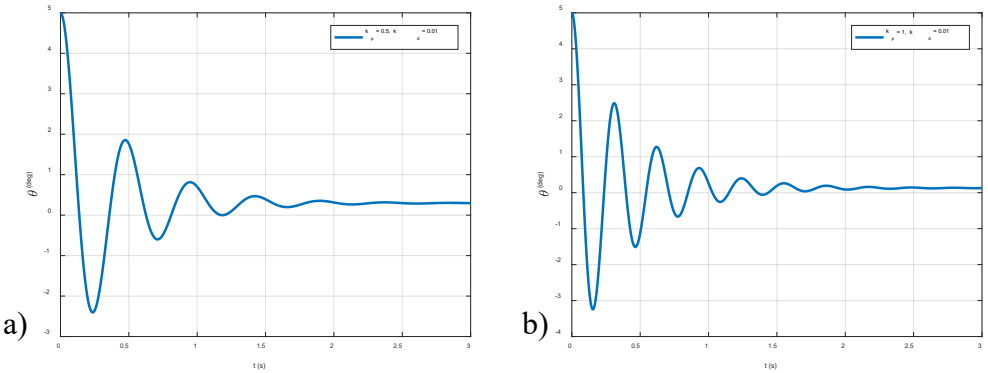

Fig. 9 Robot's inclination as function of time, for two values of k_d.

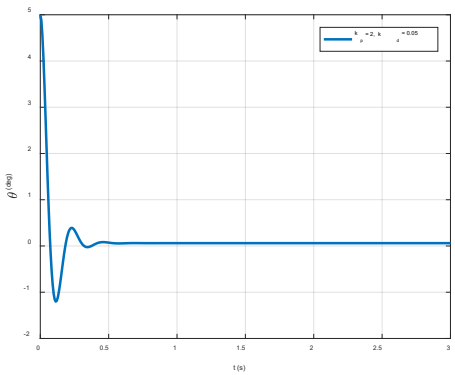

Fig. 10 Simulation of the accepted robot inclination vs. time

For example on Fig. 10 is shown the obtained $\theta(t)$ for k_p=2 Nm/rad and k_d=0.05 Nms/rad, which is the selected set of parameters implemented on the physical robot.

5. Conclusions

The possible use of two wheeled robots for space exploration has the advantage of less space for maneuvers and less energy consumption if the stability is actively controlled. In this work was investigated the inverted physical pendulum with vertical and horizontal forced motion of the slider on which is hinged the body of the robot. The Lagrange equations for these cases were deduced and numerical examples were provided. Stability domains are determined for sets frequency-force for both the vertical and horizontal harmonic forced motions.

However, rendering stable an inverted pendulum -like robot is not energy efficient and we have developed a mechanical model for a robot stabilized by a control loop.

In the case of a two-wheeled robot with controlled torque applied to the wheels, were deduced the nonlinear differential equations of motion. The PD controller was introduced in the numerical simulation and several examples were investigated. We have shown that the frequency of oscillation of the motor increases with increasing k_p and the damping of oscillations is increasing with increasing k_d. For practical reasons, were selected for the real robot, higher values for k_p and k_d which produce a strong damping (final value of the inclination is close to zero and is reached after 0.6s).

The investigated case of a TWIP robot opens the perspective of further studies for the controlled forward-backward motions and for rotations around the vertical axis.

R E F E R E N C E S

[1] *R. P. M. Chan, K. A. Stol and R. C. Halkyard*, "Review of modelling an d control of two-wheeled robots," *Annual Review in Control,* vol. 37, pp. 89-103, 2013.

[2] *D. Fuquan, G. Xueshan, J. Shigong, G. Wenzeng and L. Yubai*, "A two-wheeled inverted pendulum robot with friction compensation," *Mechatronics,* vol. 30, pp. 116-125, 2015.

[3] "designboom," Designboom, 24 May 2010. [Online]. Available: https://www.designboom.com/. [Accessed 12 March 2024].

[4] *W. Avi, F. Eli and H. B. Uri*, "Optimizing step climbing by two connected wheeled inverted pendulum robots," *Procedia Manufacturing,* vol. 21, pp. 236-242, 2018.

[5] *G. Isaac, M.-C. Jorge, S. Víctor, A.-A. Carlos and M.-V. Javier*, "Trajectory tracking control of a self-balancing robot via adaptive neural," *Engineering Science and Technology, an International Journal,* vol. 35, 2022.

[6] *P. L. Kapiza*, "Dynamic stability of a pendulum when its point of suspension vibrates," *Soviet Phys. JETP.,* vol. 21, p. 588–597, 1951.

[7] *E. I. Butikov*, "On the dynamic stabilization of an inverted pendulum," *American Journal of Physics,* vol. 69, no. 6, pp. 1-14, 2001.

[8] *E. I. Butikov*, "An improved criterion for Kapitza's pendulum," *Journal of Physics A: Mathematical and Theoretical,* vol. 44, pp. 1-16, 2011.

[9] *R. E. Grundy*, "The Kapitza equation for the inverted pendulum," *The Quarterly Journal of Mechanics and Applied Mathematics,* vol. 72, no. 2, p. 261–272, 2019.

[10] *R. Voinea, I. Stroe and M. V. Predoi*, Technical Mechanics, Bucharest: Ed. Politehnica Press, 2010.

[11] "Kapitza's pendulum," Wikipedia, 23 12 2023. [Online]. Available: https://en.wikipedia.org/wiki/Kapitza%27s_pendulum#cite_note-Kapitza-1. [Accessed 25 03 2024].

[12] "MATLAB, 1994-2017 The MathWorks, Inc.," 2017. [Online]. Available: https://www.mathworks.com/products/matlab.html. [Accessed 20 11 2017].

[13] *N. A. Stepanov and M. A. Skvortsov*, "Inverted pendulum driven by a horizontal random force: statistics of the never-falling trajectory and supersymmetry," *SciPost Phys,* vol. 13, no. 2, p. 25, 2022.